 Accepted Manuscript published as ERC-22-0251.R1. Accepted for publication: 20-Jun-2023

Chromosomal alterations in sporadic Medullary Thyroid Carcinoma and correlation with outcome

Teresa Ramone[1*], Cristina Romei[1*], Raffaele Ciampi[1], Roberta Casalini[1], Angelo Valetto[2], Veronica Bertini[2], Francesco Raimondi[3], Anthony Onoja[3], Alessandro Prete[1], Antonio Matrone[1], Carla Gambale[1], Paolo Piaggi[4], Liborio Torregrossa[5], Clara Ugolini[5], Rossella Elisei[1].

[1] Department of Clinical and Experimental Medicine, Unit of Endocrinology, University Hospital of Pisa, Pisa, Italy.
[2] Section of Cytogenetics, Department of Laboratory Medicine, University Hospital of Pisa, Pisa, Italy.
[3] Laboratorio di Biologia Bio@SNS, Scuola Normale Superiore, Pisa, Italy.
[4] Department of Information Engineering, University of Pisa, Pisa, Italy.
[5] Department of Surgical, Medical, Molecular Pathology and Critical Area, Unit of Pathology, University Hospital of Pisa, Pisa, Italy.

*these authors equally contributed to this study

Short title: Chromosomal alterations in Medullary Thyroid Carcinoma

Keywords: Somatic chromosomal number alterations, SCNA, Medullary Thyroid Carcinoma, *RET*, tumor progression

Word count: 3953

Corresponding author: Prof. Rossella Elisei Department of Clinical and Experimental Medicine, Unit of Endocrinology, University Hospital of Pisa, Pisa, Italy. Email: rossella.elisei@med.unipi.it

Abstract

Somatic Copy Number Alterations (SCNA) involving either a whole chromosome or just one of the arms, or even smaller parts have been described in about 88% of human tumors. This study investigated the SCNA profile in 40 well-characterized sporadic medullary thyroid carcinomas by comparative genomic hybridization array. We found that 26/40(65%) cases had at least one SCNA. The prevalence of SCNA, and in particular of chromosome 3 and 10, was significantly higher in cases with a *RET* somatic mutation. Similarly, SCNA of chromosomes 3, 9, 10 and 16 were more frequent in cases with a worse outcome and an advanced disease. By the pathway enrichment analysis, we found a mutually exclusive distribution of biological pathways in metastatic, biochemically persistent and cured patients. In particular, we found gain of regions involved in the intracellular signaling and loss of regions involved in DNA repair and TP53 pathways in the group of metastatic patients. Gain of regions involved in cell cycle and senescence were observed in patients with biochemical disease. Finally, gain of regions associated to the immune system and loss of regions involved in the apoptosis pathway were observed in cured patients suggesting a role of specific SCNA and corresponding altered pathways in the outcome of sporadic MTC.

 Accepted Manuscript published as ERC-22-0251.R1. Accepted for publication: 20-Jun-2023

INTRODUCTION

Human cancer is characterized by the accumulation of small DNA somatic alterations, including base substitutions, indels and structural rearrangements (Vogelstein *et al.* 2013). Somatic Copy Number Alterations (SCNA) involving either a whole chromosome (aneuploidy) or single arms, either p or q, or even smaller parts of them can be also present (Taylor *et al.* 2018). In cancer, SCNA are responsible, more than any other DNA alteration, of most genetic modifications (Beroukhim et al., 2010; Zack et al, 2013; Mitelman, 2000). The downstream effect of SCNA is still unknown, but it has been hypothesized that SCNA can alter the expression of a plethora of genes that play important roles in cancer development and progression (Shao *et al.* 2019).

The Cancer Genome Atlas (TCGA) demonstrated that approximately 88% of cancers had at least some detectable SCNA that varied across cancer types (Taylor *et al.* 2018), with many chromosomes of interest affected by SCNA, both as loss and gain. The most frequently involved chromosomes are 6p, 12q, 17q and 19q, which can be either gained or lost; chromosome arms 1q, 7p, 8q and 20q, which are mainly gained; and chromosome arms 3p, 8p, 17p, 18p, 18q and 22q, which are mainly lost (Taylor *et al.* 2018; Gao & Baudis 2021; Wen *et al.* 2021). Not all cancers have the same grade of SCNA; for example, it has been reported that SCNA is present in almost all cases of glioblastoma, while only 26% of thyroid carcinomas show SCNA (Taylor *et al.* 2018). A correlation between SCNA and the clinical characteristics of tumors has been reported, and SCNA have been shown to contribute to cancer progression and aggressiveness in prostate and breast cancer (Stopsack *et al.* 2019; Voutsadakis 2021).

Another important event observed in cancer cells is the phenomenon of chromothripsis, described as an event where chromosome pieces break apart and then reassemble in a random order. Chromothripsis has been associated with a poor outcome and with aggressive tumor behavior (Stephens *et al.* 2011).

Thyroid carcinomas are a class of tumors characterized by different histological origins and by different clinical behaviors. The majority of thyroid carcinoma is derived from follicular cells, while medullary thyroid carcinoma (MTC) is derived from parafollicular C cells. SCNA were identified in 27.2% of papillary thyroid carcinomas (PTCs) (Agrawal *et al.* 2014), while in MTC, a variable

frequency, ranging from 50 to 77%, has been reported (Frisk *et al.* 2001; Marsh *et al.* 2003; Flicker *et al.* 2012; Qu *et al.* 2020).

The present study investigated the SCNA profile in a series of well-characterized sporadic MTCs by comparative genomic hybridization array (CGH) with the aim of clarifying its prevalence and role in tumor development and biological behavior.

PATIENTS AND METHODS

Study group

MTC fresh primary tumor tissues are routinely collected at the time of thyroidectomy at the Endocrine Surgery Unit of the University Hospital of Pisa (Italy). The snap-frozen tissues are stored at -80 °C. The MTC diagnosis is confirmed by histology, and all patients are followed up for the clinical status at the Endocrine Unit of the same hospital. To the purpose of this study, we selected 40 MTC cases whose mutation profile was previously identified: 23 cases were positive and 17 negative for *RET* somatic mutation. The present study was approved by the Institutional Review Board and by the "Comitato Etico Regionale per la Sperimentazione Clinica della Regione Toscana (CEAVNO)" Prot 14387_ELISEI (20/04/2022). This study was conducted in accordance with the Declaration of Helsinki. All patients signed a written informed consent form.

DNA extraction and NGS mutation profile

DNA from fresh frozen tissue was extracted either with an automated method on a Maxwell16® (Promega, Madison, WI, USA) or with the manual DNeasy Blood and Tissue Kit (QIAGEN, Hilden, Germany). The DNA concentration was measured with a Qubit 3 fluorometer (Invitrogen, Carlsbad, CA, USA) and a QubitTM dsDNA HS Assay kit, and the purity of the DNA was assessed by measuring the 260/230 and 260/280 ratios with a Nanodrop spectrophotometer. The Ion S5 targeted next generation sequencing (NGS) method with a custom panel designed using the AmpliSeq Designer tool was applied to detect the mutation status of the MTC samples. The details of this method have been previously reported (Ciampi *et al.* 2019).

Array comparative genomic hybridization (array-CGH)

 Accepted Manuscript published as ERC-22-0251.R1. Accepted for publication: 20-Jun-2023

Two hundred nanograms of DNA was differentially labeled with Cy5-dCTP or with Cy3-dCTP using random primer labeling according to the manufacturer's protocol (Agilent Technologies, Santa Clara, California, U.S.A.). The labeling reactions were applied to the oligo-arrays and incubated for 24 h at 67 °C. Slides were washed and scanned using the Agilent scanner. Identification of individual spots on the scanned arrays and the quality evaluation of the slides were performed using Agilent dedicated software.

The array CGH was performed on a 60K SurePrint G3 Human CGH Microarray. CNVs were identified with Cytogenomics 4.0.3.12 using the Aberration Detection Method-2 algorithm (ADM-2). ADM-2 uses an iterative procedure to find all genomic intervals with a score above a user/specified statistical threshold value. The aberration threshold was set to a minimum of 6 with the minimum number of 3 probes required in a region and a minimum absolute log ratio of 0.25. We analyzed all of the alterations in the copy number that were greater than 3 contiguous probes for deletions and greater than 4 probes for duplications, independent of their absolute size; the CNVs were compared to those reported in the http://dgv.tcag.ca/variation. The gene content was established with the UCSC Genome Browser (http://genome.ucsc.edu/) (NCBI37/hg19 assembly), and the gene function was established by RefSeq (https://www.ncbi.nlm.nih.gov/refseq/rsg/).

Two DNAs used as controls were isolated from blood of normal subjects (one man and one woman) and were supplied as reagents in the labelling Kit (Agilent Technologies, Santa Clara, California, USA). Their copy number variants were known and were reported as track in the analysis software.

Bioinformatic pathway analysis

We considered all the SCNA profiles of the 40 patients. The individual patients' SCNA data were concatenated, and the patients' ID, chromosome cytobands, and aberration regions (amplified+gains versus deletion+losses) were retained to develop the feature matrix. The patients' IDs were considered the column, while their chromosomes and cytobands were considered the row observations. On the feature matrix, the amplified+gains regions had positive values (high), while the deletion+losses regions had negative values (low). We represented the somatic SCNA and mutations for each patient using the *ComplexHeatmap* library (v2.2.0) (Gu *et al.* 2016) within

the R statistical scripting language (v4.1.1). We generated a representation for specific SCNA chromosome coordinates. Each cell was colored according to the nature of the SCNA: red for loss and blue for gain. Samples were color annotated using their clinical phenotype, i.e., “Metastatic”, “Biochemical persistence” and “Cured patient”. We performed pathway enrichment analysis using Reactome web browser (Gillespie *et al.* 2022), considering oncogenes and tumor suppressor genes (TSGs) from the Cancer Gene Census (Sondka *et al.* 2018), in duplicated and deleted regions, respectively, and by grouping altered genes in distinct patient groups (i.e. “Metastatic”, “Biochemical persistence” and “Cured patient”). The False Discovery Rate (FDR) of the enriched pathways in the different groups were combined, using –log(FDR) and log(FDR) transformed values for pathways enriched in amplified/gained and deleted/lost regions, respectively. The resulting summary matrix was used to perform unsupervised clustering, using the “linkage” function from the python library *scipy.cluster.hierarchy* (v1.4.1), and the “AgglomerativeClustering” from the *sklearn.cluster* (v1.0.2) library, employing *seaborn* (v0.11.2) and “matplotlib.pyplot” libraries for heatmap visualizations, within the Python scripting language (v. 3.8.10).

Expression analysis of selected genes

We tested the expression of some genes mapping on differentially altered chromosomes (gain or loss) in metastatic and non-metastatic cases. For the amplified chromosome 16 we tested the expression of *ABBC1* and *PDPK1* genes and for the deleted chromosomes we analyzed the expression of *MLH1*, *FHIT* (chromosome 3) and *ATF4* (chromosome 22). We selected these genes because they were all reported as altered in cancer pathways (Zabarovsky *et al.* 2002; Gagliardi *et al.* 2018; Williams *et al.* 2021; Poku & Iram 2022).

Total RNA was isolated from MTC tumoral fresh tissues using the TRIzol reagent lysis buffer (Invitrogen, Carlsbad, CA) according to the protocol suggested by the manufacturer. Total RNA was quantified using the Qubit RNA HS and the Qubit fluorometer. A total of 100 ng of RNA was used to synthesize the cDNA using the SuperScript IV VILO (Thermo Fisher, Carlsbad, CA). The cDNA was diluited to a final concentration of 2 ng/ul.

Droplet digital PCR (ddPCR) was used to measure the levels of gene expression of our targets. A total of 10 ng of cDNA was used in the PCR multiplex reaction for *MLH1* (dHsaCPE5032951),

 Accepted Manuscript published as ERC-22-0251.R1. Accepted for publication: 20-Jun-2023

FHIT (dHsaCPE5042915), *ATF4* (dHsaCPE5191903) and *ABCC*1 (dHsaCPE5054680) and a duplex PCR reaction for *PDPK1* (dHsaCPE5049610) and the reference gene *HPRT1* (dHsaCPE5192872). The PCR reaction was prepared using the Multiplex Supermix (Bio-Rad Laboratories Hercules, California, USA) according to the manufacturer instructions and analyzed with the QuantaSoft analysis software version 1.1 (Bio-Rad Laboratories Hercules, California, USA). Only samples with more than 10.000 events count were included in the analysis. The level of gene expression was reported as n° of copies/ µl. The values of gene expression of the targets were normalized with the levels of HPRT1 gene expression.

Evaluation of the immune infiltration

Thirty-six MTC cases were analyzed for the presence of immune infiltration. The analysis of the immune infiltration was performed on hematoxylin-eosin-stained section representative of the tumor, using the “hot spots” method: three fields under low power magnification were selected (original magnification 5x using a standard Leica DM4000 microscope) and evaluated. The lymphocytic infiltration was graded as follows: 0 absent, 1 mild, 2 lymphoid follicles without germinal center, 3 lymphoid follicles with germinal center. Intra-tumoral and extra-tumoral lymphocyte infiltration was evaluated.

Statistical analysis

The statistical analysis was performed using the statistical tool GraphPad Prism 9.0. The correlation between chromosome alteration, mutational status and outcome was analyzed by the chi-squared test and Fisher’s test. The Kruskal–Wallis test was used for the correlation between the SCNA and the presence of metastases at diagnosis, as well as the outcomes of the MTC patients and to compare RNA expression levels in cases with amplified or deleted SCNA. A p value<0.05 was considered significant.

Results

Somatic mutational profile by NGS

The molecular characterization of the 40 selected MTC performed by NGS analysis confirmed that 23 MTC harbored a *RET* somatic mutation and in particular a p.Cys620Tyr, a p.Cys630Arg, a

p.Glu632_639delinsHisArg, a p.Glu632_Cys634del, a p.Ala883Phe, a p.Asp898_Glu901del, in single cases; a p.Cys634Arg in 2 cases and a p.Met918Thr in 15 cases. NGS also confirmed the absence of a *RET* somatic alteration in the other 17 cases (*RET*-) but also showed that 8 cases had a *HRAS* somatic mutation (p.Gly12Arg, p.Gln61Lys, p.Gln61Leu, in 1 case; p.Gly13Arg in 2 cases and p.Gln61Arg in 3 cases) while the remaining 9 cases did not show any other somatic mutations among those analyzed with our panel (Ciampi *et al.* 2019).

SCNA as detected by Array-CGH and according to the somatic *RET* mutations

The array CGH results have been illustrated in Figure 1. Twenty-six cases (26/40, 65%) had at least one SCNA (SCNA number range per sample: from 1 to 27), and 14 cases (14/40, 35%) did not show any SCNA. In general, chromosome losses (n=91 events) were more frequent than chromosome gains (n=50 events). SCNA (either loss or gain events) involved both whole chromosomes (41 events of whole chromosome loss and 21 events of whole chromosome gain) or only the p or q arm of specific chromosomes. We found 50 partial chromosome losses and 29 partial chromosome gains. As shown in Figure 1, the chromosomes most frequently involved in SCNA were chromosome 22 (32.5% of cases), chromosome 1 (30% of cases), chromosome 3 (20% of cases), chromosome 10 (17.5% of cases), chromosome 21 (15% of cases), and chromosomes 4, 9, 16 and 17 (12.5% of cases). Four patients, all *RET* positive, were affected by the chromothripsis phenomenon: two cases on chromosome 10, one on chromosome 11 and one on chromosome 17. The remaining chromosomes were affected by only a few SCNA. A detailed representation of the cytobands affected by SCNA is shown in Figure 2.

The prevalence of SCNA was analyzed according to the presence of the somatic *RET* mutation. As shown in Figure 3 Panel A, among the 23 *RET*+ MTC tissues, 18/23 (78.3%) had at least one SCNA, while only 8/17 *RET*- tissues (47%) showed at least one SCNA (p=0.05). Moreover, in terms of the number of SCNA present in the tissues, there was also a statistically significant difference between the mean number of SCNA in *RET*+ tissues (mean±SD: 5.13±7.21) and *RET*- tissues (mean±SD: 0.92±1.83) (p=0.03) (Fig. 3, Panel B).

 Accepted Manuscript published as ERC-22-0251.R1. Accepted for publication: 20-Jun-2023

Since most of *RET* positive cases had the p.Met918Thr mutation, we did not find any statistically significant association between the mean number of SCNA among cases with different types of *RET* mutation (i.e. p.Met918Thr, n=15 and other *RET* mutations, n=8).

Correlation of SCNA with clinical characteristics

We evaluated the correlation of SCNA with the clinical features of the tumor (i.e., the absence of metastases, presence of lymph node metastases and distant metastases) at diagnosis and with the outcome (i.e., metastatic disease vs. biochemical disease and no disease) of the patients at the end of follow-up. The correlation analysis was performed only for patients for whom clinical data were available (n=38). As shown in Figure 4A, we found that the number of SCNA was higher in patients who presented distant metastases at diagnosis with respect to those who had only lymph node metastases or no metastases at all (p=0.035). We also found that the number of SCNA was higher in patients who had metastatic disease with respect to those who were cured or those who showed only biochemical disease at the end of follow up (p=0.014) (Fig. 4B).

Identification of chromosomes specifically associated with the outcome and *RET* somatic mutations

We compared the prevalence of the presence of any kind of SCNA for each chromosome in MTC tissues according to the patients' outcome (i.e., presence of metastases, biochemical persistent disease- and disease-free patients at the end of follow up) (Table 1) and to the presence of *RET* somatic mutations (Table 2). A statistically significant association was observed between alterations on chromosomes 3, 9, 10 and 16 and the outcome being the SCNA of these chromosomes more frequent in metastatic cases respect to the others (p=0.0009, p=0.02, p=0.02 and p=0.02, respectively). Despite chromosomes 1 and 22 were the most frequently altered in our series no differences in the prevalence of their SCNA have bene found in the three categories of patients' outcome.

The same type of analysis was performed by looking at the *RET+* and *RET-* cases. As reported in Table 2, a significantly higher number of SCNA on chromosomes 3 and 10 (p=0.01 and p=0.01, respectively) was found in the *RET+* group respect to the *RET-* group.

Pathway enrichment analysis

We performed a pathway analysis by assessing the enrichment of either oncogenes or tumor suppressor genes (TSG) in the gain and loss regions, respectively, and we compared the results obtained among metastatic, biochemically persistent, and cured patients (Fig. 5). A mutually exclusive distribution of biological pathways was observed according to the outcome of the patients.

In the group of metastatic patients, we observed a SCNA gain of chromosomal regions that included genes involved in intracellular signaling by second messenger and signal transduction pathways and a SCNA loss of chromosomal regions that included genes involved in DNA repair and in gene expression and transcriptional regulation by TP53 pathways.

In the group of patients with biochemical disease, we observed a SCNA gain of chromosomal regions that included genes involved in the cell cycle, cellular response to stimuli, senescence, metabolism of RNA and the regulation of gene expression pathways.

In the group of cured patients, we observed a SCNA gain of chromosomal regions that included genes associated with the Tall Like Receptor signaling cascade, immune system and death receptor signaling pathways and a SCNA loss of chromosomal regions that included genes associated with the apoptosis pathway.

Gene expression analysis

We analyzed the expression of *ABCC1, PDPK1, MLH1*, *FHIT and ATF4* in a total of 20 samples: Table 3 reports the number of aneuploid (gain and loss) and diploid cases studied for each gene.

When we compared the RNA expression of *ABCC1, PDPK1, MLH1* and *FHIT* genes we found a clear tendency of correlation between SCNA and gene expression but not a real statistical

 Accepted Manuscript published as ERC-22-0251.R1. Accepted for publication: 20-Jun-2023

significance (data not shown). At variance, the RNA of *ATF4* gene was statistically less expressed in deleted cases (p=0.05) (Fig. 6).

Analysis of lymphocytic infiltration

To verify the hypothesis that cured patients had an enriched immune system, as resulted by the enrichment pathway analysis, we analyzed the presence of lymphocytic infiltration in 36/40 MTC cases. Intra-tumoral lymphocytic infiltration was found at low level only in 3 cases and was not considered for the analysis. Extra-tumoral infiltration was observed in 16 cases (grade 1,2 or 3) but not in the other 20 cases (grade=0). Although not statistically significant, we observed a higher level of lymphocytic infiltration in cured patients (data not shown).

Discussion

Human cancer has been demonstrated to be largely affected by SCNA (Beroukhim *et al.* 2010), which correlates with patient prognosis (Zack *et al.* 2013). Recently, 10,729 tumors (across 32 cancer types) were analyzed by Harbers et al., and 87.5% of them (28/32) were affected by SCNA; in particular, ovarian cancer and sarcoma were the cancer types with the highest number of chromosome alterations (Harbers *et al.* 2021). Although it is still not clear how SCNA contribute to the tumorigenesis process, SCNA could alter the expression levels of genes involved in chromosome gain and loss (Santaguida & Amon 2015), and they are considered hallmarks of cancer, similar to somatic mutations.

In keeping with pancancer data, thyroid tumors were also characterized by SCNA (Herrmann 2003; Liu *et al.* 2013). Among the different histotypes of thyroid cancer, SCNA has also been described in MTC, with different results for SCNA being reported at a variable frequency ranging from 50%-77% (Frisk *et al.* 2001; Marsh *et al.* 2003; Flicker *et al.* 2012; Qu *et al.* 2020).

In our group, 65% of tumors were affected by at least one SCNA, in agreement with both the already reported SCNA prevalence in MTC and the rate (67.9%) of chromosome aberrations reported in solid tumors (Duijf *et al.* 2013). When we evaluated the prevalence of losses versus gains of chromosome regions, we found that chromosome losses were more frequent than gains

(91 vs. 50 events, respectively), as has also been generally observed by Duijf et al., who analyzed several types of solid tumors (Duijf *et al.* 2013).

In the present series, as well as in that reported by other authors (Frisk *et al.* 2001; Ye *et al.* 2008), SCNA was identified in both *RET*+ and *RET*- cases. We found a statistically significant higher prevalence of cases with SCNA in the *RET*+ group. This finding is in line with our previous studies showing a higher prevalence of chromosome 10 variations in *RET*+ cases (Ciampi *et al.* 2012; Ramone *et al.* 2020) and further supports the hypothesis that the *RET* mutation may confer genomic instability at least to chromosome 10. On this regard it is worth to say that we found similar results, at least for chromosome 10, although by using different methodologies. To our knowledge, this statistical significant association has not been reported in previous studies either because only the p.Met918Thr *RET* mutation has been searched for (Frisk *et al.* 2001) and because both sporadic and hereditary MTC have been included (Ye *et al.* 2008). We recently demonstrated that *RET*-mutated C-cells grow and proliferate more rapidly than nonmutated cells (Romei *et al.* 2021). In keeping with this observation, we could hypothesize that due to the higher proliferation rate of *RET*+ cells and the consequent cell divisions, a progressive accumulation of genetic events might occur and, among them, also many SCNA that, once they occur, can contribute to the progression of the disease.

The correlation of SCNA with clinical outcomes has been reported in other human tumors, such as prostate and lung tumors (Hieronymus *et al.* 2018; Kou *et al.* 2021). In the present series, a higher prevalence of SCNA was observed in MTC tissues of patients with a more advanced tumor at diagnosis and with a worse clinical outcome, as already shown in a previously reported MTC series (Frisk *et al.* 2001) and in other human tumors (Fallenius *et al.* 1988; Hemmer *et al.* 1997; Torres *et al.* 2007). In fact, the amplification of chromosomal regions containing oncogenes involved in tumor progression or the loss of regions containing TSG could justify the correlation between SCNA and metastatic progression and poor outcomes of the disease (Bloomfield & Duesberg 2016). A strong correlation between SCNA and gene expression has been found, demonstrating upregulation of the levels of expression of genes that map to gained regions and downregulation of levels of expression of genes that map to lost regions (Shao *et al.* 2019). This evidence has been partially

 Accepted Manuscript published as ERC-22-0251.R1. Accepted for publication: 20-Jun-2023

confirmed in our series; indeed, the expression level of 4/5 analyzed genes (i.e., *ABCC1*, *PDPK1, MLH1, FHIT*) was not statistically different between aneuploid and diploid cases, although showing a tendency of correlation. The only one that showed a statistically significant correlation between its RNA expression and the SCNA was ATF4. One possible explanation is that the absence of statistical difference could be due to the small number of aneuploid cases analyzed for the expression of *ABCC1*, *PDPK1, MLH1, FHIT* while *ATF4*, that was the only one that we could analyze on 8 aneuploid vs 12 diploid cases, reached the statistical significance.

SCNA occur on different chromosomes, but specific regions have been associated with a poor outcome (Ach *et al.* 2013; Park *et al.* 2014; Koçak *et al.* 2020). In our group of study, we observed that although different chromosomes were affected by SCNA, chromosomes 3, 9, 10 and 16 were preferentially altered in patients with a metastatic outcome, suggesting that they could have a potential role in tumor evolution. In addition, SCNA on chromosomes 3 and 10 were preferentially altered in *RET*+ cases.

In agreement with other studies on MTC (Hemmer *et al.* 1999; Frisk *et al.* 2001; Marsh *et al.* 2003; Ye *et al.* 2008), we also observed that chromosome 3 was very frequently completely or partially lost, and it is worth noting that many TSGs involved in cancer pathways map to chromosome 3 (Zabarovsky *et al.* 2002; Ingvarsson 2005; Angeloni 2007; Hesson *et al.* 2007). Some authors hypothesize that the loss of genes involved in TERT transcriptional regulation, which are located on the p arm of chromosome 3, could explain its major role in tumor development (Yagyu *et al.* 2021).

A similar mechanism of involvement could be hypothesized for chromosome 9, which in our series was totally lost only in metastatic patients. The loss of chromosome 9 is an event previously described in MTC (Frisk *et al.* 2001; Marsh *et al.* 2003; González-Yebra *et al.* 2012), and it is associated with a poor outcome in some tumors (Di Nunno *et al.* 2019). Moreover, Han et al. demonstrated that the loss of 9p21 confers primary resistance to immune checkpoint therapy (Han *et al.* 2021), thus potentially explaining why immunotherapy did not show relevant results in *RET*+ tumors, at least so far (Hegde *et al.* 2020).

We observed both losses and gains on chromosome 10, where the *RET* gene maps (10q11.21). As reported in our previous study (Ramone *et al.* 2020), the *RET* gene, and more generally chromosome 10, SCNA is a sporadic event in sMTC, with a positive correlation with the presence of a somatic *RET* mutation and its Variant Allele Frequency (VAF). Additionally, in this study, we confirmed that an alteration of *RET* via SCNA is not an alternative event to a *RET* somatic mutation but rather an additional event that could enhance the role of this driver mutation in tumor progression, since SCNA on chromosome 10 is correlated with a worse outcome of the disease.

Although the losses were more represented in our series, chromosome 16 was gained but interestingly only in metastatic patients. Except for one case with only long arm gain, the remaining cases had amplification of the whole chromosome. Likely, oncogenes that map to this chromosome being amplified could contribute to cancer evolution, and this hypothesis is also supported by literature data that suggest a correlation between chromosome 16 gain and a poor clinical outcome in different types of cancer (Mampaey *et al.* 2015; Bramhecha *et al.* 2018).

Although not significantly correlated with the outcome or *RET* somatic mutations, we observed that chromosome 22 was frequently lost in our cases of sMTC. Notably, the *ATF4* gene, which is a negative regulator of *RET*, maps to chromosome 22, and the loss of the *ATF4* gene is associated with shorter survival, especially in association with *RET* p.Met918Thr (Williams *et al.* 2021).

SCNA involves different chromosomes, but the pathways and, more specifically, the genes affected by this alteration are poorly defined. Taking advantage of the latest technique's analysis and bioinformatic tools, we performed a pathway enrichment analysis that demonstrated different and mutually exclusive pathway activations in MTC tissues of patients with different outcomes. In the group of metastatic patients, we observed an SCNA gain of chromosomal regions that included genes involved in intracellular signaling and signal transduction. These findings are in keeping with the evidence that an enrichment of genes involved in cellular proliferation and differentiation as well as the MAPKinase and PI3kinase pathways strengthens the role of these genes in tumor development and progression (Garraway & Lander 2013).

In the same group, we observed a loss of those pathways involved in the mechanism of DNA repair, whose deficiency could be compatible with tumor progression (Knijnenburg *et al.* 2018).

 Accepted Manuscript published as ERC-22-0251.R1. Accepted for publication: 20-Jun-2023

This pathway ensures genomic stability and integrity (Olave & Graham 2022), but its inactivation (for example, due to genomic loss) could further induce an already neoplastic cell to accumulate other errors. One of the genes that belongs to this pathway is *MLH1*, whose genomic location is on chromosome 3 (3p22.2) that, as said, was associated with a poor outcome in our cases.

Mutually exclusive pathways were found to be altered, although at a lower rate, in the other two groups of patients. In particular, it is worth noting that the presence of SCNA gain of chromosomal regions, including genes associated with the immune system pathway, was present only in the group of cured patients. This evidence has been confirmed also at tissue level where a not statistically significant but higher presence of lymphocytic infiltration has been observed in cured patients respect to the biochemical and metastatic patients. This finding could be in keeping with a role of the immune system in the control of tumor development and progression as shown in some human tumors. Nevertheless, additional studies are needed to confirm this interesting observation.

Conclusions

In conclusion, we found a higher prevalence of SCNA in sporadic MTC comparable to that of other solid tumors. SCNA are more frequent and more numerous in MTC tissues harboring a somatic *RET* mutation. Some specific chromosomal SCNA had a correlation with an advanced stage at diagnosis and with patients' outcomes. Peculiar and mutually exclusive pathway alterations were found in three groups of patients when distinguished according to their outcome, suggesting a role of specific SCNA and corresponding altered pathways in the metastatic progression of sporadic MTC or in its definitive cure.

Conflicts of Interest: The authors declare that there are no conflicts of interest that could affect the impartiality of the reported research.

Funding: This study has been supported by grant to R.E. from Associazione Italiana per la Ricerca sul Cancro (AIRC, Investigator grant 2018, project code 21790).

Acknowledgements The manuscript has been revised by the American Journal Experts for language.

Authors' contribution: TR, CR, RE, RC were responsible for designing the research, extracting and analysing data, interpreting results and writing the report. TR, RC, AV, VB were involved in bench work. FR, AO, PP performed the statistical evaluation of data and in the pathways analysis. AP, AM, LT contributed to the selection of patients to be included in the study and to the clinical data evaluation.

 Accepted Manuscript published as ERC-22-0251.R1. Accepted for publication: 20-Jun-2023

Legend of figures

Figure 1: Oncoprint of chromosomes affected by SCNA in MTC cases. Each column represents a patient, and each row represents a chromosome. The colored squares indicate the presence of an SCNA: blue for a gain, red for a loss. The number in the square represents the number of alterations in that chromosome. The histograms above the figure indicate the number of SCNA on all chromosomes for each case. On the right of the oncoprint, there are 2 columns: the first column (n°) indicates how many times each chromosome is altered in the group of 40 cases, and the second column indicates the percentage (%). Mutation profile is reported at the bottom of the figure: green squares indicate the presence of a *RET* p.Met918Thr mutation; pink squares indicates *RET* mutation other than p.Met918Thr; gray squares indicate *RET*- cases (including also RAS positive cases).

Figure 2: A detailed representation of the cytobands affected by SCNA in the group of cases with at least one alteration (n=26). Each column indicates a cytoband; each row indicates an sMTC case. In the right part of the figure, we report the outcome and the somatic mutation profile of the patients. All colors reported in the oncoprint are explained in the legend. Specific cytobands are put in order from right to left according to the higher prevalence of alterations.

Figure 3: Correlation of SCNA and *RET* mutation. Panel A) Graphical representation of the percentage of patients with or without SCNA in the *RET*+ and *RET*- groups: the percentage of patients with a higher number of SCNA was greater in the *RET*+ group than in the *RET*- group. Panel B) Mean number of SCNA in the *RET*+ and *RET*- groups: the cases that harbored a *RET* mutation had a much higher mean number of SCNA than the *RET*- cases. The differences were considered statistically significant when the P value was less than 0.05.

Figure 4: Correlation between SCNA and clinical features. Comparison between SCNA and the presence of metastases at diagnosis (Panel A) and between SCNA and the outcome of the patients (Panel B). Differences were considered statistically significant when the P value was less than 0.05.

Figure 5: Pathway enrichment analysis visualization: hierarchical clustering and heatmap representation of top 15 most significantly enriched Reactome pathways (FDR < 0.01) in the genes

affected by SCNA found in either metastatic, biochemical, or cured patients. We restricted our analysis to oncogenes in amplified or gained regions and tumor suppressor genes (TSG) in deleted or lost regions. Pathways enriched in chromosome gains and chromosome losses are reported in blue and red, respectively. The color intensity is proportional to –log(FDR) and log(FDR) for pathways enriched in amplified/gained and deleted/lost regions, respectively.

Figure 6: Correlation of *ATF4* gene expression levels between diploid and loss cases. Expression levels are indicated as the ratio between the expression level of the target gene and of the housekeeping gene (*HPRT1*) both expressed as number of copies/μl.

 Accepted Manuscript published as ERC-22-0251.R1. Accepted for publication: 20-Jun-2023

Bibliography

Ach T, Zeitler K, Schwarz-Furlan S, Baader K, Agaimy A, Rohrmeier C, Zenk J, Gosau M, Reichert TE, Brockhoff G *et al.* 2013 Aberrations of MET are associated with copy number gain of EGFR and loss of PTEN and predict poor outcome in patients with salivary gland cancer. *Virchows Archiv: An International Journal of Pathology* **462** 65–72. (doi:10.1007/s00428-012-1358-0)

Agrawal N, Akbani R, Aksoy BA, Ally A, Arachchi H, Asa SL, Auman JT, Balasundaram M, Balu S, Baylin SB *et al.* 2014 Integrated Genomic Characterization of Papillary Thyroid Carcinoma. *Cell* **159** 676–690. (doi:10.1016/j.cell.2014.09.050)

Angeloni D 2007 Molecular analysis of deletions in human chromosome 3p21 and the role of resident cancer genes in disease. *Briefings in Functional Genomics & Proteomics* **6** 19–39. (doi:10.1093/bfgp/elm007)

Beroukhim R, Mermel CH, Porter D, Wei G, Raychaudhuri S, Donovan J, Barretina J, Boehm JS, Dobson J, Urashima M *et al.* 2010 The landscape of somatic copy-number alteration across human cancers. *Nature* **463** 899–905. (doi:10.1038/nature08822)

Bloomfield M & Duesberg P 2016 Inherent variability of cancer-specific aneuploidy generates metastases. *Molecular Cytogenetics* **9** 90. (doi:10.1186/s13039-016-0297-x)

Bramhecha YM, Guérard K-P, Rouzbeh S, Scarlata E, Brimo F, Chevalier S, Hamel L, Dragomir A, Aprikian AG & Lapointe J 2018 Genomic Gain of 16p13.3 in Prostate Cancer Predicts Poor Clinical Outcome after Surgical Intervention. *Molecular Cancer Research: MCR* **16** 115–123. (doi:10.1158/1541-7786.MCR-17-0270)

Ciampi R, Romei C, Cosci B, Vivaldi A, Bottici V, Renzini G, Ugolini C, Tacito A, Basolo F, Pinchera A *et al.* 2012 Chromosome 10 and RET gene copy number alterations in hereditary and sporadic Medullary Thyroid Carcinoma. *Molecular and Cellular Endocrinology* **348** 176–182. (doi:10.1016/j.mce.2011.08.004)

Ciampi R, Romei C, Ramone T, Prete A, Tacito A, Cappagli V, Bottici V, Viola D, Torregrossa L, Ugolini C *et al.* 2019 Genetic Landscape of Somatic Mutations in a Large Cohort of Sporadic Medullary Thyroid Carcinomas Studied by Next-Generation Targeted Sequencing. *IScience* **20** 324–336. (doi:10.1016/j.isci.2019.09.030)

Di Nunno V, Mollica V, Brunelli M, Gatto L, Schiavina R, Fiorentino M, Santoni M, Montironi R, Caliò A, Eccher A *et al.* 2019 A Meta-Analysis Evaluating Clinical Outcomes of Patients with Renal Cell Carcinoma Harboring Chromosome 9P Loss. *Molecular Diagnosis & Therapy* **23** 569–577. (doi:10.1007/s40291-019-00414-0)

Duijf PHG, Schultz N & Benezra R 2013 Cancer cells preferentially lose small chromosomes. *International Journal of Cancer* **132** 2316–2326. (doi:10.1002/ijc.27924)

Fallenius AG, Franzén SA & Auer GU 1988 Predictive value of nuclear DNA content in breast cancer in relation to clinical and morphologic factors. A retrospective study of 227 consecutive cases. *Cancer* **62** 521–530. (doi:10.1002/1097-0142(19880801)62:3<521::aid-cncr2820620314>3.0.co;2-f)

Flicker K, Ulz P, Höger H, Zeitlhofer P, Haas OA, Behmel A, Buchinger W, Scheuba C, Niederle B, Pfragner R *et al.* 2012 High-resolution analysis of alterations in medullary thyroid carcinoma genomes. *International Journal of Cancer* **131** E66–E73. (doi:10.1002/ijc.26494)

Frisk T, Zedenius J, Lundberg J, Wallin G, Kytölä S & Larsson C 2001 CGH alterations in medullary thyroid carcinomas in relation to the RET M918T mutation and clinical outcome. *International Journal of Oncology* **18** 1219–1225. (doi:10.3892/ijo.18.6.1219)

Gagliardi PA, Puliafito A & Primo L 2018 PDK1: At the crossroad of cancer signaling pathways. *Seminars in Cancer Biology* **48** 27–35. (doi:10.1016/j.semcancer.2017.04.014)

Gao B & Baudis M 2021 Signatures of Discriminative Copy Number Aberrations in 31 Cancer Subtypes. *Frontiers in Genetics* **12** 654887. (doi:10.3389/fgene.2021.654887)

Garraway LA & Lander ES 2013 Lessons from the cancer genome. *Cell* **153** 17–37. (doi:10.1016/j.cell.2013.03.002)

Gillespie M, Jassal B, Stephan R, Milacic M, Rothfels K, Senff-Ribeiro A, Griss J, Sevilla C, Matthews L, Gong C *et al.* 2022 The reactome pathway knowledgebase 2022. *Nucleic Acids Research* **50** D687–D692. (doi:10.1093/nar/gkab1028)

González-Yebra B, Peralta R, González AL, Ayala-Garcia MA, de Zarate MEMO & Salcedo M 2012 Genetic alterations in a primary medullary thyroid carcinoma and its lymph node metastasis in a patient with 15 years follow-up. *Diagnostic Pathology* **7** 63. (doi:10.1186/1746-1596-7-63)

Gu Z, Eils R & Schlesner M 2016 Complex heatmaps reveal patterns and correlations in multidimensional genomic data. *Bioinformatics (Oxford, England)* **32** 2847–2849. (doi:10.1093/bioinformatics/btw313)

Han G, Yang G, Hao D, Lu Y, Thein K, Simpson BS, Chen J, Sun R, Alhalabi O, Wang R *et al.* 2021 9p21 loss confers a cold tumor immune microenvironment and primary resistance to immune checkpoint therapy. *Nature Communications* **12** 5606. (doi:10.1038/s41467-021-25894-9)

Harbers L, Agostini F, Nicos M, Poddighe D, Bienko M & Crosetto N 2021 Somatic Copy Number Alterations in Human Cancers: An Analysis of Publicly Available Data From The Cancer Genome Atlas. *Frontiers in Oncology* **11** 700568. (doi:10.3389/fonc.2021.700568)

Hegde A, Andreev-Drakhlin AY, Roszik J, Huang L, Liu S, Hess K, Cabanillas M, Hu MI, Busaidy NL, Sherman SI *et al.* 2020 Responsiveness to immune checkpoint inhibitors versus other systemic therapies in RET-aberrant malignancies. *ESMO Open* **5** e000799. (doi:10.1136/esmoopen-2020-000799)

Hemmer J, Thein T & Van Heerden WF 1997 The value of DNA flow cytometry in predicting the development of lymph node metastasis and survival in patients with locally recurrent oral squamous cell carcinoma. *Cancer* **79** 2309–2313. (doi:10.1002/(sici)1097-0142(19970615)79:12<2309::aid-cncr3>3.0.co;2-g)

Hemmer S, Wasenius VM, Knuutila S, Franssila K & Joensuu H 1999 DNA copy number changes in thyroid carcinoma. *The American Journal of Pathology* **154** 1539–1547. (doi:10.1016/S0002-9440(10)65407-7)

Herrmann M 2003 Standard and molecular cytogenetics of endocrine tumors. *American Journal of Clinical Pathology* **119 Suppl** S17-38. (doi:10.1309/C97C-7EY0-0KRQ-WYVT)

Hesson LB, Cooper WN & Latif F 2007 Evaluation of the 3p21.3 tumour-suppressor gene cluster. *Oncogene* **26** 7283–7301. (doi:10.1038/sj.onc.1210547)

 Accepted Manuscript published as ERC-22-0251.R1. Accepted for publication: 20-Jun-2023

Hieronymus H, Murali R, Tin A, Yadav K, Abida W, Moller H, Berney D, Scher H, Carver B, Scardino P *et al.* 2018 Tumor copy number alteration burden is a pan-cancer prognostic factor associated with recurrence and death. *ELife* **7** e37294. (doi:10.7554/eLife.37294)

Ingvarsson S 2005 Tumor Suppressor Genes on Human Chromosome 3 and Cancer Pathogenesis. *Cancer Genomics & Proteomics* **2** 247–253.

Knijnenburg TA, Wang L, Zimmermann MT, Chambwe N, Gao GF, Cherniack AD, Fan H, Shen H, Way GP, Greene CS *et al.* 2018 Genomic and Molecular Landscape of DNA Damage Repair Deficiency across The Cancer Genome Atlas. *Cell Reports* **23** 239-254.e6. (doi:10.1016/j.celrep.2018.03.076)

Koçak A, Heselmeyer-Haddad K, Lischka A, Hirsch D, Fiedler D, Hu Y, Doberstein N, Torres I, Chen W-D, Gertz EM *et al.* 2020 High Levels of Chromosomal Copy Number Alterations and TP53 Mutations Correlate with Poor Outcome in Younger Breast Cancer Patients. *The American Journal of Pathology* **190** 1643–1656. (doi:10.1016/j.ajpath.2020.04.015)

Kou F, Wu L, Guo Y, Zhang B, Li B, Huang Z, Ren X & Yang L 2021 Somatic copy number alterations are predictive of progression-free survival in patients with lung adenocarcinoma undergoing radiotherapy. *Cancer Biology & Medicine* j.issn.2095-3941.2020.0728. (doi:10.20892/j.issn.2095-3941.2020.0728)

Liu Y, Cope L, Sun W, Wang Y, Prasad N, Sangenario L, Talbot K, Somervell H, Westra W, Bishop J *et al.* 2013 DNA copy number variations characterize benign and malignant thyroid tumors. *The Journal of Clinical Endocrinology and Metabolism* **98** E558-566. (doi:10.1210/jc.2012-3113)

Mampaey E, Fieuw A, Van Laethem T, Ferdinande L, Claes K, Ceelen W, Van Nieuwenhove Y, Pattyn P, De Man M, De Ruyck K *et al.* 2015 Focus on 16p13.3 Locus in Colon Cancer. *PloS One* **10** e0131421. (doi:10.1371/journal.pone.0131421)

Marsh DJ, Theodosopoulos G, Martin-Schulte K, Richardson A-L, Philips J, Röher H-D, Delbridge L & Robinson BG 2003 Genome-wide copy number imbalances identified in familial and sporadic medullary thyroid carcinoma. *The Journal of Clinical Endocrinology and Metabolism* **88** 1866–1872. (doi:10.1210/jc.2002-021155)

Olave MC & Graham RP 2022 Mismatch repair deficiency: The what, how and why it is important. *Genes, Chromosomes & Cancer* **61** 314–321. (doi:10.1002/gcc.23015)

Park HS, Jang MH, Kim EJ, Kim HJ, Lee HJ, Kim YJ, Kim JH, Kang E, Kim S-W, Kim IA *et al.* 2014 High EGFR gene copy number predicts poor outcome in triple-negative breast cancer. *Modern Pathology: An Official Journal of the United States and Canadian Academy of Pathology, Inc* **27** 1212–1222. (doi:10.1038/modpathol.2013.251)

Poku VO & Iram SH 2022 A critical review on modulators of Multidrug Resistance Protein 1 in cancer cells. *PeerJ* **10** e12594. (doi:10.7717/peerj.12594)

Qu N, Shi X, Zhao J-J, Guan H, Zhang T-T, Wen S-S, Liao T, Hu J-Q, Liu W-Y, Wang Y-L *et al.* 2020 Genomic and Transcriptomic Characterization of Sporadic Medullary Thyroid Carcinoma. *Thyroid: Official Journal of the American Thyroid Association* **30** 1025–1036. (doi:10.1089/thy.2019.0531)

Ramone T, Mulè C, Ciampi R, Bottici V, Cappagli V, Prete A, Matrone A, Piaggi P, Torregrossa L, Basolo F *et al.* 2020 RET Copy Number Alteration in Medullary Thyroid Cancer Is a Rare Event Correlated with RET Somatic Mutations and High Allelic Frequency. *Genes* **12** 35. (doi:10.3390/genes12010035)

Romei C, Ramone T, Mulè C, Prete A, Cappagli V, Lorusso L, Torregrossa L, Basolo F, Ciampi R & Elisei R 2021 RET mutated C-cells proliferate more rapidly than non-mutated neoplastic cells. *Endocrine Connections* **10** 124–130. (doi:10.1530/EC-20-0589)

Santaguida S & Amon A 2015 Short- and long-term effects of chromosome mis-segregation and aneuploidy. *Nature Reviews. Molecular Cell Biology* **16** 473–485. (doi:10.1038/nrm4025)

Shao X, Lv N, Liao J, Long J, Xue R, Ai N, Xu D & Fan X 2019 Copy number variation is highly correlated with differential gene expression: a pan-cancer study. *BMC Medical Genetics* **20** 175. (doi:10.1186/s12881-019-0909-5)

Sondka Z, Bamford S, Cole CG, Ward SA, Dunham I & Forbes SA 2018 The COSMIC Cancer Gene Census: describing genetic dysfunction across all human cancers. *Nature Reviews. Cancer* **18** 696–705. (doi:10.1038/s41568-018-0060-1)

Stephens PJ, Greenman CD, Fu B, Yang F, Bignell GR, Mudie LJ, Pleasance ED, Lau KW, Beare D, Stebbings LA *et al.* 2011 Massive genomic rearrangement acquired in a single catastrophic event during cancer development. *Cell* **144** 27–40. (doi:10.1016/j.cell.2010.11.055)

Stopsack KH, Whittaker CA, Gerke TA, Loda M, Kantoff PW, Mucci LA & Amon A 2019 Aneuploidy drives lethal progression in prostate cancer. *Proceedings of the National Academy of Sciences of the United States of America* **116** 11390–11395. (doi:10.1073/pnas.1902645116)

Taylor AM, Shih J, Ha G, Gao GF, Zhang X, Berger AC, Schumacher SE, Wang C, Hu H, Liu J *et al.* 2018 Genomic and Functional Approaches to Understanding Cancer Aneuploidy. *Cancer Cell* **33** 676-689.e3. (doi:10.1016/j.ccell.2018.03.007)

Torres L, Ribeiro FR, Pandis N, Andersen JA, Heim S & Teixeira MR 2007 Intratumor genomic heterogeneity in breast cancer with clonal divergence between primary carcinomas and lymph node metastases. *Breast Cancer Research and Treatment* **102** 143–155. (doi:10.1007/s10549-006-9317-6)

Vogelstein B, Papadopoulos N, Velculescu VE, Zhou S, Diaz LA & Kinzler KW 2013 Cancer genome landscapes. *Science (New York, N.Y.)* **339** 1546–1558. (doi:10.1126/science.1235122)

Voutsadakis IA 2021 The Landscape of Chromosome Instability in Breast Cancers and Associations with the Tumor Mutation Burden: An Analysis of Data from TCGA. *Cancer Investigation* **39** 25–38. (doi:10.1080/07357907.2020.1863418)

Wen X, Cimera R, Aryeequaye R, Abhinta M, Athanasian E, Healey J, Fabbri N, Boland P, Zhang Y & Hameed M 2021 Recurrent loss of chromosome 22 and SMARCB1 deletion in extra-axial chordoma: A clinicopathological and molecular analysis. *Genes, Chromosomes & Cancer* **60** 796–807. (doi:10.1002/gcc.22992)

Williams MD, Ma J, Grubbs EG, Gagel RF & Bagheri-Yarmand R 2021 ATF4 loss of heterozygosity is associated with poor overall survival in medullary thyroid carcinoma. *American Journal of Cancer Research* **11** 3227–3239.

Yagyu T, Ohira T, Shimizu R, Morimoto M, Murakami Y, Hanaki T, Kihara K, Matsunaga T, Yamamoto M, Tokuyasu N *et al.* 2021 Human chromosome 3p21.3 carries TERT transcriptional regulators in pancreatic cancer. *Scientific Reports* **11** 15355. (doi:10.1038/s41598-021-94711-6)

Ye L, Santarpia L, Cote GJ, El-Naggar AK & Gagel RF 2008 High resolution array-comparative genomic hybridization profiling reveals deoxyribonucleic acid copy number alterations associated with

 Accepted Manuscript published as ERC-22-0251.R1. Accepted for publication: 20-Jun-2023

medullary thyroid carcinoma. *The Journal of Clinical Endocrinology and Metabolism* **93** 4367–4372. (doi:10.1210/jc.2008-0912)

Zabarovsky ER, Lerman MI & Minna JD 2002 Tumor suppressor genes on chromosome 3p involved in the pathogenesis of lung and other cancers. *Oncogene* **21** 6915–6935. (doi:10.1038/sj.onc.1205835)

Zack TI, Schumacher SE, Carter SL, Cherniack AD, Saksena G, Tabak B, Lawrence MS, Zhsng C-Z, Wala J, Mermel CH *et al.* 2013 Pan-cancer patterns of somatic copy number alteration. *Nature Genetics* **45** 1134–1140. (doi:10.1038/ng.2760)

Table 1: Correlation between the outcome of sporadic MTC patients and SCNA in different chromosomes.

	Tissues with SNCA N (%)			
	Metastatic disease (N=16) n (%)	*Biochemical disease (N=7) n (%)*	*Disease free (N=15) n (%)*	*P value**
Chr 1	6 (37.5)	2 (28.6)	4 (26.7)	0.8
Chr 2	3 (18.7)	0	0	0.1
Chr 3	8 (50)	0	0	**0.0009**
Chr 4	3 (18.7)	0	2 (13.3)	0.5
Chr 5	1 (6.2)	0	0	0.5
Chr 6	2 (12.5)	0	0	0.2
Chr 7	3 (18.7)	0	0	0.1
Chr 8	2 (12.5)	0	2 (13.3)	0.6
Chr 9	5 (31.2)	0	0	**0.02**
Chr 10	6 (37.5)	1 (14.3)	0	**0.02**
Chr 11	2 (12.5)	0	0	0.2
Chr 12	2 (12.5)	0	0	0.2
Chr 13	3 (18.7)	0	0	0.1
Chr 14	3 (18.7)	0	1 (6.7)	0.3
Chr 15	2 (12.5)	0	2 (13.3)	0.6
Chr 16	5 (31.2)	0	0	**0.02**
Chr 17	4 (25)	0	1 (6.7)	0.2
Chr 18	2 (12.5)	0	0	0.6
Chr 19	2 (12.5)	0	0	0.2
Chr 20	2 (12.5)	0	0	0.2
Chr 21	4 (25)	1 (14.3)	1 (6.7)	0.4
Chr 22	8 (50)	3 (42.8)	2 (13.3)	0.08
Chr X	2 (12.5)	0	1 (6.7)	0.58
Chr Y	2 (12.5)	0	1 (6.7)	0.6

* We used chi-squared test and differences were considered statistically significant when the P-value was less than 0.05.

 Accepted Manuscript published as ERC-22-0251.R1. Accepted for publication: 20-Jun-2023

Table 2: Number of *RET+* and *RET-* patients presenting SCNA in different chromosomes.

	SNCA N (%)		
	RET+ cases (N=23) n (%)	*RET- cases (N=17) n (%)*	*p-value**
Chr 1	8 (34.8)	4 (23.5)	0.5
Chr 2	3 (13)	0	0.2
Chr 3	8 (34.8)	0	**0.01**
Chr 4	3 (13)	2 (11,7)	0.9
Chr 5	2 (8.7)	0	0.5
Chr 6	2 (8.7)	0	0.5
Chr 7	2 (8.7)	1 (5.9)	0.7
Chr 8	4 (17.4)	0	0.1
Chr 9	5 (21.7)	0	0.05
Chr 10	7 (30.4)	0	**0.01**
Chr 11	2(8.7)	0	0.5
Chr 12	2 (8.7)	0	0.5
Chr 13	3 (13)	0	0.2
Chr 14	2 (8.7)	1(5.9)	0.7
Chr 15	2 (8.7)	2 (11,7)	0.7
Chr 16	4 (17.4)	1 (5.9)	0.4
Chr 17	3 (13)	2 (11,7)	1
Chr 18	2 (8.7)	0	0.5
Chr 19	2 (8.7)	0	0.5
Chr 20	2(8.7)	0	0.5
Chr 21	4 (17.4)	3 (17.6)	1
Chr 22	10 (43.5)	3 (17.6)	0.08
Chr X	2 (8.7)	1(5.9)	0.7
Chr Y	2 (8.7)	1(5.9)	0.7

* We used Fisher test and differences were considered statistically significant when the P-value was less than 0.05.

Table 3: Cases analyzed by ddPCR for gene expression

		Diploid	***Aneuploid***	
Gene	*Cytoband*	*Diploid cases (n)*	*Loss cases (n)*	*Gain cases (n)*
MLH1	3p22.2	16	4	0
FHIT	3p14.2	16	4	0
ABCC1	16p13.11	16	0	4
PDPK1	16p13.3	16	0	4
ATF4	22q13.1	12	8	0

Accepted Manuscript published as ERC-22-0251.R1. Accepted for publication: 20-Jun-2023

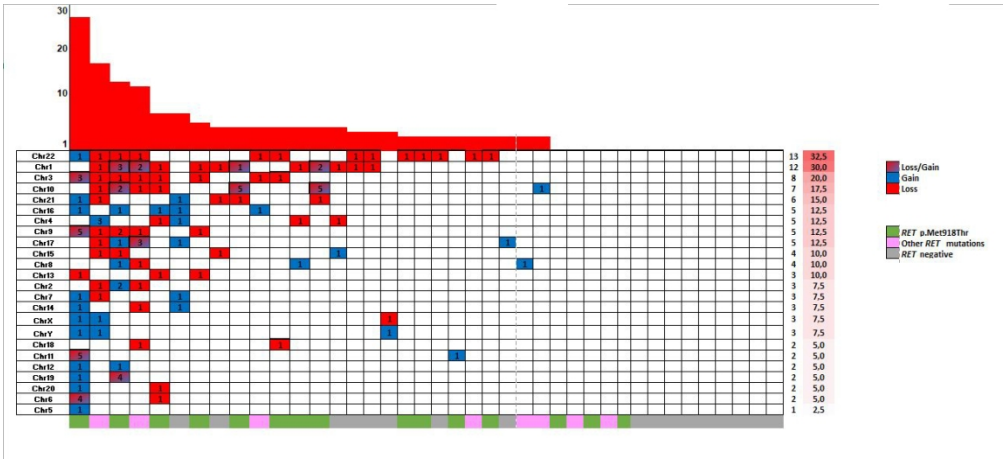

Figure 1

343x156mm (96 x 96 DPI)

Figure 2

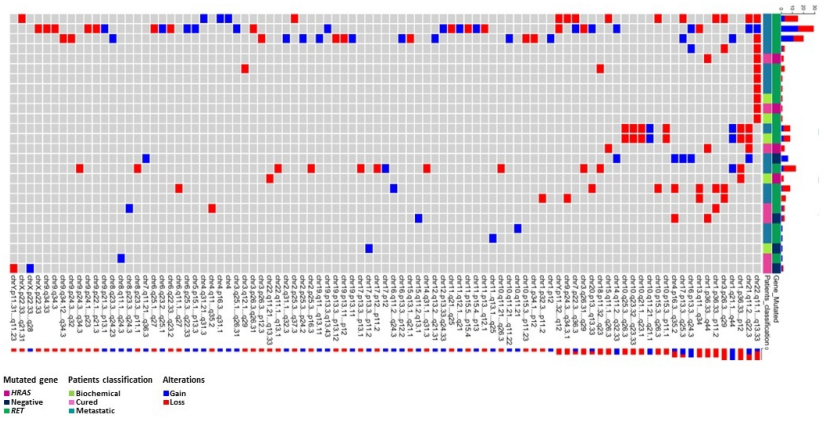

Figure 2

338x190mm (96 x 96 DPI)

Accepted Manuscript published as ERC-22-0251.R1. Accepted for publication: 20-Jun-2023

Figure 3

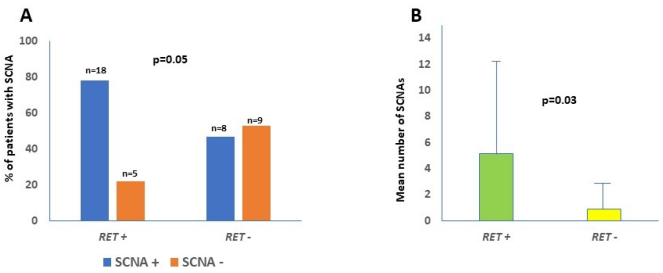

Figure 3

338x190mm (96 x 96 DPI)

Figure 4

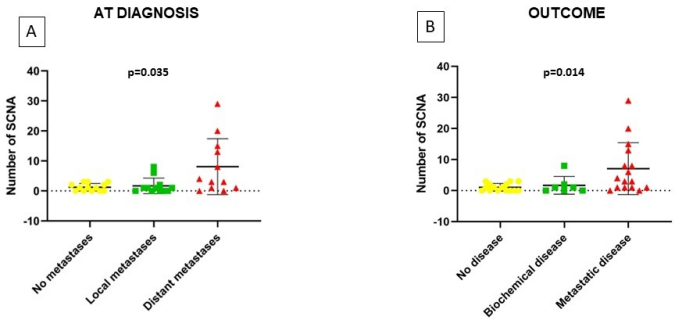

Figure 4

338x190mm (96 x 96 DPI)

Accepted Manuscript published as ERC-22-0251.R1. Accepted for publication: 20-Jun-2023

FIG 5

Figure 5

338x190mm (96 x 96 DPI)

Fig. 6

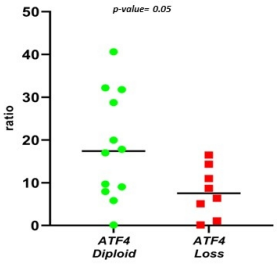

Figure 6

338x190mm (96 x 96 DPI)